

Quantum computation with quasiparticles of the Fractional Quantum Hall Effect

D.V. Averin and V.J. Goldman

Department of Physics and Astronomy, SUNY, Stony Brook, NY 11794-3800, U.S.A.

(November 14, 2018)

We propose an approach that enables implementation of anyonic quantum computation in systems of antidots in the two-dimensional electron liquid in the FQHE regime. The approach is based on the adiabatic transfer of FQHE quasiparticles in the antidot systems, and uses their fractional statistics to perform quantum logic. Advantages of our scheme over other semiconductor-based proposals of quantum computation include the energy gap in the FQHE liquid that suppresses decoherence, and the topological nature of quasiparticle statistics that makes it possible to entangle two quasiparticles without their direct dynamic interaction.

I. INTRODUCTION

“Topological” quantum computation with anyons has been suggested as a way of implementing intrinsically fault-tolerant quantum computation^{1–4}. Intertwining of anyons, quasiparticles of two-dimensional electron system (2DES) with non-trivial exchange statistics, induces unitary transformations of the system wavefunction that depend only on the topological order of the underlying 2DES. These transformations can be used to perform quantum logic, the topological nature of which is expected to make it more robust against environmental decoherence. The aim of this work is to propose specific and experimentally feasible approach for implementation of basic elements of the anyonic quantum computation using adiabatic transport of the fractional quantum Hall effect (FQHE) quasiparticles in systems of quantum antidots⁵.

An antidot is a small hole in the 2DES produced by electron depletion, which localizes FQHE quasiparticles at its boundary due to combined action of the magnetic field and the electric field created in the depleted region. If the antidot is sufficiently small, the energy spectrum of the antidot-bound quasiparticle states is discrete, with finite excitation energy Δ . When Δ is larger than the temperature T , modulation of external gate voltage can be used to attract quasiparticles one by one to the antidot^{5,6}. In this regime, adiabatic transport of individual quasiparticles in the multi-antidot systems can be used to perform quantum logic, in close analogy to adiabatic transport of individual Cooper pairs in systems of small superconducting islands in the Coulomb blockade regime⁷. In what follows, we describe specific designs of such logic gates, and discuss parameters of the FQHE qubits and mechanisms of decoherence in antidot systems.

II. FQHE QUBITS AND LOGIC GATES

As in the Cooper-pair qubits^{7–9}, information in the FQHE qubits can be encoded by the position of a quasi-

particle in the system of two antidots. The *FQHE qubit* (Fig. 1) is then the double-antidot system gate-voltage tuned near the resonance, where the energy difference ε between the quasiparticle states localized at the two antidots is small, $\varepsilon \ll \Delta$. At energies smaller than Δ , dynamics of such double-antidot system is equivalent to the dynamics of a common two-state system (qubit). The quasiparticle states localized at the two antidots are the $|0\rangle$ and $|1\rangle$ states of the computational basis of this qubit. The gate electrodes of the structure can be designed to control separately the energy difference ε and the tunnel coupling Ω of the resonant quasiparticle states.

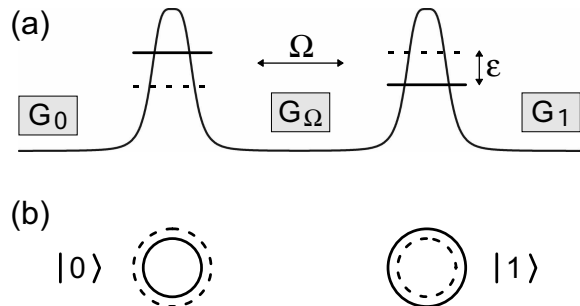


FIG. 1. Schematic energy profile (a) and structure (b) of the double-antidot FQHE qubit. Solid (dashed) lines (in (a), the horizontal lines) indicate the edges of the incompressible electron liquid when the quasiparticle is localized at the right (left) antidot. Displacement of the electron liquid is quantized due to quantization of the single-particle states circling the antidots. Dashed rectangles in (a) are the gate electrodes controlling the energies of the antidot states ($G_{0,1}$) and their tunnel coupling (G_Ω).

The most natural approach to construction of the *two-qubit gates* with the FQHE qubits is to use fractional statistics^{10,11} of the FQHE quasiparticles. Due to this statistics, intertwining of the two quasiparticle trajectories in the course of time evolution of the two qubits realizes controlled-phase transformation with non-trivial value of the phase. Precise result of this operation depends on the nature of the FQHE state. In this work, we discuss the most basic and robust Laughlin state with

the filling factor $\nu = 1/m = 1/3$, where the quasiparticles have abelian statistics and intertwining of trajectories leads to multiplication of the state wavefunction by the phase factor $e^{\pm 2\pi i/3}$. The sign of the phase depends on the direction of the magnetic field and the direction of rotation of one quasiparticle trajectory around another.

A possible structure of the controlled-phase gate is shown in Fig. 2. Each of the columns of four antidots contains two qubits, and arrows denote trajectory of quasiparticle transfer through the system. The transfer leads to transformation of the quantum state of the two qubits and its shift from the gate input (left column in Fig. 2) to the output (right column). The quasiparticle transfer can be achieved by the standard adiabatic level-crossing dynamics. If a pair of antidots is coupled by the tunnel amplitude Ω , a gate-voltage induced variation of the energy difference ε through the value $\varepsilon = 0$ (slow on the time scale Ω^{-1}) leads to the transfer of a quasiparticle between these antidots. Correct operation of the controlled-phase gate in Fig. 2 requires that the gate voltage pulses applied to the antidots are timed so that the state of the upper qubit is propagated at first halfway through the gate, then the state of the lower qubit is propagated through the whole gate, and finally the state of the upper qubit is transferred to the output. In this case, if the quasiparticle of the upper qubit is in the state $|1\rangle$, trajectories of the quasiparticle propagation in the lower qubit encircle this quasiparticle, and the two states of the lower qubit acquire an additional phase difference $\pm 2\pi/3$, conditioned on the state of the upper qubit. We take the direction of magnetic field to be such that the state $|1\rangle$ of the lower qubit acquires a positive extra phase $2\pi/3$. Assuming that parameters of the driving pulses are adjusted in such a way that the dynamic phases accumulated by the qubit states are the multiple integers of 2π , the transformation matrix P of the gate can be written as

$$P = \text{diag}[1, 1, 1, e^{2\pi i/3}] \quad (1)$$

in the basis of the four gate states $|00\rangle, |01\rangle, |10\rangle, |11\rangle$.

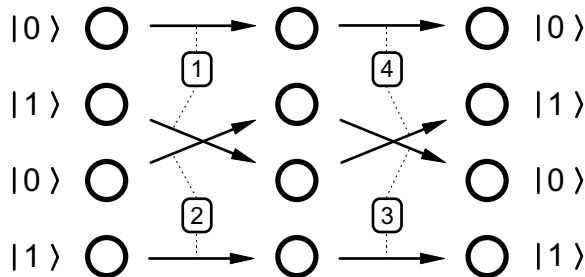


FIG. 2. A twelve-antidot two-quasiparticle implementation of the two-qubit controlled-phase gate. The states $|0\rangle$ and $|1\rangle$ are the computational basis states of the two qubits. The arrows show the quasiparticle transfer steps for each basis state during the gate operation. The arrow numbering denotes the time sequence of these steps.

Controlled-phase gate (1) combined with the possibility of performing arbitrary single-qubit transformations is sufficient for universal quantum computation. To demonstrate this explicitly, we construct a combination of the gate (1) with single-qubit gates that reproduces the usual controlled-NOT (C-NOT) gate C . The C-NOT gate is known to be sufficient for universal quantum computation¹². Since the gates P and C are not equivalent with respect to single-qubit transformations, two applications of P are required to reproduce C ¹³. To find appropriate single-qubit transformations that should complement the two P 's, it is convenient to first reduce P to the conditional z -rotation R of the second qubit through angle $-\pi/3$, $R = \text{diag}[1, 1, e^{-i\pi/3}, e^{i\pi/3}]$. We notice that $R = S(-\pi/3)P$, where $S(\alpha)$ is an unconditional shift of the phase of the state $|1\rangle$ of the first qubit by α . After this reduction, it is straightforward to find the necessary single-qubit transformations from the requirements that the state of the first qubit is unchanged by C , while the conditional action of C on the second qubit is given by the Pauli matrix σ_x . These two requirements do not specify the necessary transformations uniquely. One possible choice is to use the transformations that correspond physically to modulation of the tunnel coupling between the states of the second qubit (i.e., involve only matrices σ_x, σ_y). In this case, we obtain

$$C = S(\pi/2)U_-^\dagger S(-\pi/3)PU_-U_+S(-\pi/3)PU_+^\dagger, \quad (2)$$

where $U_\pm = [\hat{1}]_1 \otimes [\exp\{-i\varphi(\sigma_x \pm \sigma_y)/\sqrt{2}\}]_2$. Here the subscripts 1, 2 denote the part of the transformation acting on the first and the second qubit, respectively, and the rotation angle φ is given by the condition $\cos 2\varphi = 1/\sqrt{3}$, $\varphi \in [0, \pi/2]$. Physically, the transformations S can be implemented as pulses of the gate voltage applied to the antidot $|1\rangle$ of the first qubit, while U s represent pulsed modulation of the amplitude of the tunnel coupling between the two antidots of the second qubit that keeps the phase of this coupling fixed.

III. DECOHERENCE MECHANISMS

At low temperatures, the energy gap in the FQHE liquid exponentially suppresses quasiparticle excitations in the bulk of the sample. Due to this suppression, only sample edges and external metallic gate electrodes support low-energy excitations that can give rise to dissipation and decoherence in the antidot qubits. Qubit is coupled to both the gate electrodes and the edges by the Coulomb interaction. The charge q of the qubit quasiparticle (for the primary Laughlin FQHE liquids, $q = e/m$, where m is an odd integer) induces a polarization charge on the gate electrodes that oscillates in the course of qubit time evolution. The current induced in this way in the electrodes with finite resistance R leads to energy dissipation and decoherence. This decoherence mechanism associated with “electromagnetic environment” of

the structure (see, e.g.,¹⁴) is generic for most of the solid-state qubits. In the FQHE qubits, its strength should be lower than in other charge-based qubits, due to the smaller charge of the FQHE quasiparticles. Indeed, if the gate electrode is close to an antidot (on the scale of the distance d between the two qubit antidots), the amplitude of the variations of the induced charge is roughly equal to the quasiparticle charge q . In this “worst-case” scenario, the limitation on the quality factor of qubit dynamics introduced by the gate electrode is equal to $e^2 R/\hbar m^2$ and is on the order of 10^{-3} for realistic values of the resistance R and for $m = 3$ qubits considered in this work. Optimization of the gate structure of the qubit should further reduce the strength of this type of decoherence by reducing electrostatic gate-qubit coupling.

Coulomb interaction also couples qubit dynamics to edge excitations of the FQHE liquid. The edge supports one-dimensional (1D) chiral plasmon modes¹⁵ propagating with velocity v . In the situation of interest here, when the qubit-edge distance L is much larger than the qubit size d , the coupling operator V can be expressed directly in terms of the 1D density $\rho(x)$ of charge carried by plasmon modes: $V = \sigma_z \int dx U(x)\rho(x)$. In this expression, σ_z represents the position of the quasiparticle on one or the other antidot of the qubit, and $U(x)$ is the variation (with the quasiparticle position) of the electrostatic potential created by the qubit at point x along the edge. A representative estimate of dissipation/decoherence rate introduced by this coupling is given by the decay rate Γ of the excited antisymmetric superposition of the antidot states. Assuming that the qubit dipole is perpendicular to a straight edge, and that the electric field is not screened between the edge and the qubit, we can find Γ directly:

$$\Gamma = \left(\frac{d}{L}\right)^2 \left(\frac{e^2}{4\epsilon\epsilon_0\hbar v}\right)^2 \frac{\Omega}{2\pi\hbar m^3} e^{-L\Omega/\hbar v}. \quad (3)$$

Here ϵ is the material dielectric constant. This equation shows that the edge-related limitation $\hbar\Gamma/\Omega$ on the qubit quality factor can vary widely depending on the system geometry and qubit energy parameters. For a realistic set of numbers, $\epsilon \simeq 10$, $v \simeq 10^5$ m/s, $\Omega \simeq 0.1$ K, $d \simeq 100$ nm (see the discussion below), we have $\hbar\Gamma/\Omega \simeq 10^{-3}$ for the edge that is $L \simeq 3$ μ m away from the qubit.

IV. ESTIMATES AND DISCUSSION

The basic set of conditions necessary for correct operation of the FQHE qubits and gates described above can be summarized as $T \ll \epsilon$, $\Omega \ll \Delta$. The antidot excitation energy Δ is estimated as $\Delta \simeq \hbar u/r$, where r is the antidot radius and $u \simeq 10^4 \div 10^5$ m/s is the velocity of quasiparticle motion around the antidot¹⁶. This means that at a temperature $T \simeq 0.05$ K the radius r should be smaller than 100 nm. Since the tunnel coupling Ω decreases rapidly with the tunneling distance s

between the antidots, $\Omega \propto \exp\{-eBs^2/12\hbar\}$ ¹⁷, the fact that it should remain at least larger than T means that the distance between the tunnel-coupled antidots should not exceed few magnetic lengths $l = (\hbar/eB)^{1/2} \simeq 10$ nm for typical values of the magnetic field B . Although these requirements on the radius r and antidot spacing s can be satisfied with the present-day fabrication technology, the necessity to control these parameters accurately presents a formidable challenge. It should be noted that this situation is not specific to our FQHE scheme, but characterizes all semiconductor solid-state qubits based directly on the quantum dynamics of individual quasiparticles, and not collective degrees of freedom (used, e.g., in the case of superconductors).

We believe that the challenges in fabrication of the FQHE qubits are well compensated for by the advantages of the FQHE approach. First of them is the energy gap of the FQHE liquid that suppresses quasiparticle excitations and associated decoherence in the bulk of the 2DES, and allows to control the remaining sources of decoherence through the system layout – see the discussion above. The second advantage is the topological nature of statistical phase that makes it possible to entangle qubits without their direct dynamic interaction. This should lead to a simpler design of the FQHE quantum logic circuit in comparison to other solid-state qubits, where control of the qubit-qubit interaction typically presents a difficult problem.

ACKNOWLEDGMENTS

This work was supported by the NSA and ARDA under the ARO contract.

¹ A.Yu. Kitaev, quant-ph/9707021.

² J. Preskill, in: *Introduction to quantum computation and information*, Eds. H.-K. Lo, S. Pappas, and T. Spiller, (World Scientific, 1998), p. 213.

³ S. Lloyd, quant-ph/0004010.

⁴ M.H. Freedman, A.Yu. Kitaev, M.J. Larsen, and Z. Wang, quant-ph/0101025.

⁵ V.J. Goldman and B. Su, *Science* **267**, 1010 (1995).

⁶ I.J. Maasilta and V.J. Goldman, *Phys. Rev. Lett.* **84**, 1776 (2000).

⁷ D.V. Averin, *Solid State Commun.* **105**, 657 (1998).

⁸ Yu. Makhlin, G. Schön, and A. Shnirman, *Nature* **398**, 305 (1999).

⁹ Y. Nakamura, Yu.A. Pashkin, and J.S. Tsai, *Nature* **398**, 786 (1999).

¹⁰ B.I. Halperin, *Phys. Rev. Lett.* **52**, 1583 (1984).

¹¹ D. Arovas, J.R. Schrieffer, and F. Wilczek, *Phys. Rev. Lett.* **53**, 722 (1984).

- ¹² A. Barenco *et al.* *Phys. Rev. A* **52**, 1583 (1995).
- ¹³ Yu. Makhlin, quant-ph/0002045.
- ¹⁴ G.-L. Ingold and Yu.V. Nazarov, in: *Single Charge Tunneling*, Eds. H. Grabert and M. Devoret (Plenum, NY, 1992), p. 21.
- ¹⁵ X.G. Wen, *Int. J. Mod. Phys. B* **6**, 1711 (1992).
- ¹⁶ I.J. Maasilta and V.J. Goldman, *Phys. Rev. B* **57**, R4273 (1998).
- ¹⁷ A. Auerbach, *Phys. Rev. Lett.* **80**, 817 (1998).